

Leveraging Large Language Models for Robot 3D Scene Understanding

William Chen, Siyi Hu, Rajat Talak, and Luca Carlone

Abstract—Semantic 3D scene understanding is a problem of critical importance in robotics. While significant advances have been made in spatial perception, robots are still far from having the common-sense knowledge about household objects and locations of an average human. We thus investigate the use of large language models to impart common sense for scene understanding. Specifically, we introduce three paradigms for leveraging language for classifying rooms in indoor environments based on their contained objects: (i) a zero-shot approach, (ii) a feed-forward classifier approach, and (iii) a contrastive classifier approach. These methods operate on 3D scene graphs produced by modern spatial perception systems. We then analyze each approach, demonstrating notable zero-shot generalization and transfer capabilities stemming from their use of language. Finally, we show these approaches also apply to inferring building labels from contained rooms and demonstrate our zero-shot approach on a real environment. All code can be found at https://github.com/MIT-SPARK/11m_scene_understanding.

I. INTRODUCTION

3D scene understanding is a key challenge in robotics. If robots are to see widespread deployment, then they must be able to not only map and localize in many environments, but also have a semantic understanding of said environments and the entities within them. If a robot is told to “go to the kitchen and fetch a spoon,” it should know what objects are usually present within kitchens and use that knowledge to figure out where to go to find one.

These aspects are typically inferred using metric-semantic simultaneous localization and mapping (SLAM) algorithms, wherein a robotic agent maps its environment, determines its location within it, and annotates the map with semantic information [1]. Modern spatial perception systems, like Kimera [2] and Hydra [3], arrange this data in 3D scene graphs – data structures wherein nodes represent locations and entities (e.g., buildings, rooms, and objects), while edges represent spatial relationships (see Fig. 1). Nodes can hold geometric information (like position and bounding box) for entities and places in the scene. However, attaching semantic labels to these nodes still remains a major open obstacle, especially for nodes corresponding to high-level spatial concepts, like rooms and buildings. To label a room node, the system must consider what objects are in the room (e.g., if it contains a stove, the room is likely a kitchen). This necessitates a “common-sense” mechanism to provide such knowledge.

The authors are affiliated with the Laboratory for Information and Decision Systems at the Massachusetts Institute of Technology, {verityw, siyi, talak, lcarlone}@mit.edu. This work was partially funded by ARL DCIST CRA W911NF-17-2-0181, ONR RAIDER N00014-18-1-2828, and Lockheed Martin Corporation’s Neural Prediction in 3D Dynamic Scene Graphs program. We also thank Prof. Jacob Andreas for his valuable inputs and Nathan Hughes for his contributions to the real experiments.

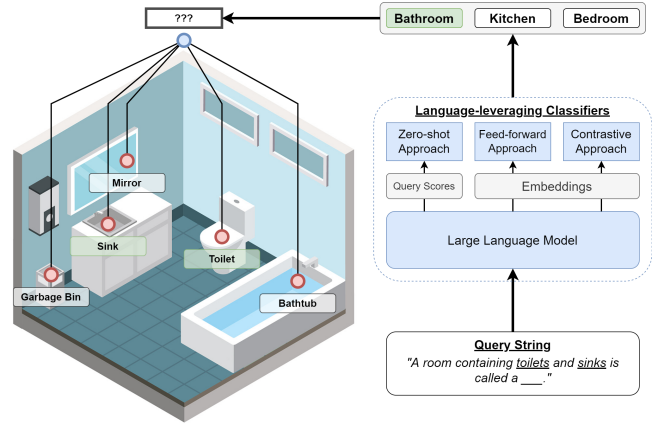


Fig. 1. 3D scene graph example. We use language models to attach high-level labels (rooms or buildings) to nodes using lower-level information.

One largely unexplored candidate method for imparting this common sense is by using language models. As they are trained on large text corpora, they capture some of the semantic information within said datasets – e.g., a language model may learn that the sentence “Bathrooms contain ___” is better finished with “toilets” rather than “stoves,” thereby containing some of the common sense needed for scene understanding. Furthermore, being what [4], [5] famously called an “infinite use of finite means,” language allows arbitrary common-sense queries to be compactly made and evaluated, including ones with novel concepts and entities. This is important for spatial perception, as *deployed robots will naturally come across many objects that engineers did not expect during development*. Being able to do inference over novel object types would thus be highly beneficial.

In this work, we look at using language models as a general tool for inferring high-level semantics (room labels) from lower-level primitives (the objects within). Specifically, we use language to describe the contents of a room, then use language models to either perform zero-shot inference of which room label best fits the description *or* embed the description as an input for task-specific classifiers. Our methods leverage the latent common sense within language models, either during evaluation or when creating semantically-meaningful embeddings, so they are able to generalize to unfamiliar objects and require no/limited training. We also show these approaches’ applicability by using them for inferring *building* labels from contained rooms and for inferring room labels on actual 3D scene graphs from [3].

II. RELATED WORKS

Metric-Semantic SLAM. As high-level semantic understanding is vital for human-robot interaction and planning,

there has been significant interest in combining classical methods with deep learning for metric-semantic SLAM. Such works generally focus on low-level representations, such as object-centric approaches [1], [6], [7], [8], dense approaches [9], [10], [11], or a hybrid of the two [12], [13]. However, these methods generally disregard higher-level semantic labeling, such as for rooms and buildings, which are needed for many planning and reasoning tasks.

Hierarchical Mapping and Building Parsing. An alternative approach is to consider hierarchical maps, which represent the robot’s environment at different levels of abstraction. Works like [14], [15] divide robot knowledge into spatial and semantic information, then anchoring the former to the latter. Our work focuses on scene graphs as a hierarchical map representation. Such data structures were first commonly used for labeling and entity relationship detection tasks in images [16], [17], but have since been generalized to 3D, where they have found success in robotics and vision [18], [19], [2], [3]. Nevertheless, anchoring semantics to spatial information in 3D scene graphs remains difficult, motivating us to look towards language models.

Language and Robotics. Using language models for semantic reasoning has been a rapidly-expanding area of research. Recent works generally focus on question answering [20], fact completion [21], [22], and logical reasoning [23]. Previous robotics papers like [24], [25], [26], [27], [28], [29], [30], [31] have mainly leveraged language for communicating goals or instructions to a robot to plan around or execute. To the best of our knowledge, natural language processing tools have not been used for robot scene understanding or room classification. Past works like [32] instead use an explicit Bayesian probabilistic framework for determining room labels based on detected objects. This work also classifies based off the most common objects in a room. However, these methods remain hard to generalize to new rooms and objects, requiring co-occurrence statistics to be collected for each additional one. In hopes of addressing these shortcomings and capitalizing on the benefits of language, in this project, we explore the ability for large language models to be used as common-sense mechanisms for robot scene understanding.

III. LANGUAGE MODELS FOR ROOM AND BUILDING CLASSIFICATION

We present three frameworks for identifying room labels based on the contained objects (and buildings based on contained rooms). All algorithms operate on 3D scene graphs akin to the ones produced by [2], [3]. At their core, all three methods summarize a room’s contents in a query sentence, then process the sentence in the following ways:

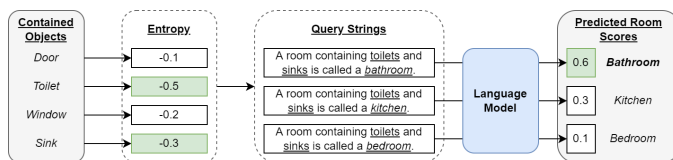


Fig. 2. Example of zero-shot approach.

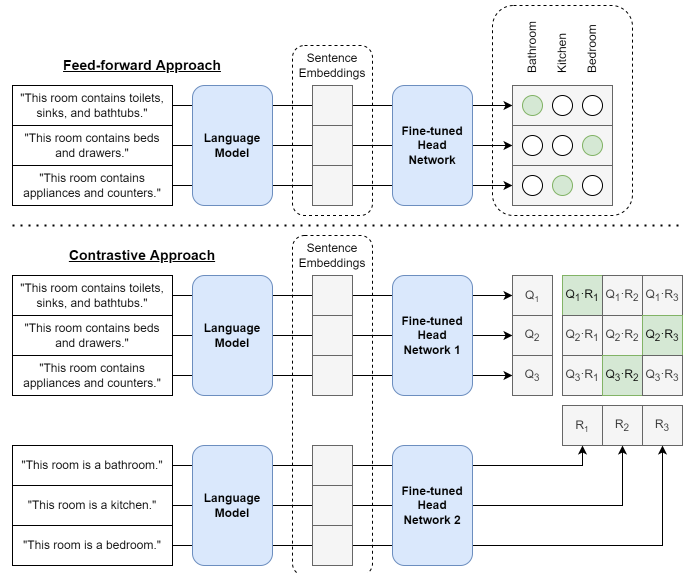


Fig. 3. Example of the two fine-tuning-based approaches: feed-forward (top) and contrastive (bottom).

- **Zero-shot:** A pre-trained language model scores which room label is best described by the query.
- **Feed-forward:** The query string is embedded by a pre-trained language model. Then, a fine-tuned neural network outputs a distribution over room labels given that embedding.
- **Contrastive:** The query *and* room label strings are embedded and transformed into a shared high-dimensional space by fine-tuned neural networks, where corresponding query-label pairs are mapped close together.

A. Language Model Capabilities

Language models are commonly broken into two types: *masked language models* (MLMs) like BERT [33] and RoBERTa [34] and *next-token prediction models*, like GPT variants [35], [36], [37]. Both types are able to score a string W based off of semantic and grammatical sensibility. For MLMs, this can be done with pseudo-log likelihoods [38]. For next-token prediction models, the model estimates W ’s log probability, $\log p(W)$. Returning to the example in Sec. I, we expect a sentence like “Bathrooms contain toilets.” to be scored higher than “Bathrooms contain stoves.” We thus use the scores of strings containing common-sense facts as a proxy measure for how likely it is for the fact to be true.

Language models can also embed texts into high-dimensional vectors that summarize the texts’ meaning and grammar. These embeddings are often used as inputs to task-specific model heads [39]. We denote the language model mapping from strings W to summary embeddings as $\Lambda(W)$.

B. Query Strings and Informative Objects

We start by building query strings describing a given room whose label we wish to infer. For this, we assume access to a list of objects within each room. This list can be inferred by existing metric-semantic SLAM techniques [2], [3]. For

our experiments, we use the ground truth object labels from our considered dataset (see Sec. IV-A).

Putting *all* objects in a room into the query may result in poor performance, as the queries may be dominated by uninformative, ubiquitous objects (e.g., lights and doors). We thus select only the k most semantically informative objects, noting that *objects which appear in fewer room types are more informative*, since their presence heavily implies certain room labels. Quantitatively, these objects have more *non-uniform* distributions $p(r_j | o_i)$, where $o_i \in L_O$ is the object label, $r_j \in L_R$ is the room label, and $L_{R,O}$ are the sets of room and object labels respectively. We compute these conditional probabilities in two ways:

- **Using ground-truth co-occurencies**, i.e., finding how many times each object label appears in each type of room and normalizing over rooms. However, this does need task-specific data. When using these empirical conditionals, we apply Laplace smoothing.
- **Using proxy co-occurency probabilities by querying language models**. Specifically, we use:

$$p(r_j | o_i) \approx \frac{\text{explog } p(W_{o_i, r_j})}{\sum_{r_j' \in L_R} \text{explog } p(W_{o_i, r_j'})} \quad (1)$$

where W_{o_i, r_j} is the query string “A room containing o_i is called a(n) r_j .” and $\log p(W_{o_i, r_j})$ is computed via language model (see Sec. III-A).

In either case, with $p(r_j | o_i)$ available, a natural measure of its non-uniformity is entropy:

$$H_{o_i} = - \sum_{r_j \in L_R} p(r_j | o_i) \log p(r_j | o_i) \quad (2)$$

Entropy is maximized when the considered distribution is uniform and minimized when it is one-hot, meaning more semantically-informative objects have *lower* corresponding H_{o_i} values. Thus, to pick objects for the queries, we take the k different lowest-entropy present objects:

$$O_{\text{best}} = \arg \min_{o_i \in O} k [H_{o_i}] \quad (3)$$

where O is the set of all object labels contained within the considered room. We thus now have a set of k objects O_{best} which can be used to infer the room label.

C. Zero-shot Approach

For the zero-shot approach, we construct $|L_R|$ query strings, one per room label:

$$W_{r_j} = \text{“A room containing } o_1, o_2, \dots \text{ and } o_k \text{ is called a(n) } r_j\text{.” } \forall r_j \in L_R \quad (4)$$

where $o_{1..k} \in O_{\text{best}}$ are ordered by ascending entropy. All these queries are scored via language model, with the final estimated room label \hat{r} being whichever one yields the highest query sentence probability:

$$\hat{r} = \arg \max_{r_j} \log p(W_{r_j}) \quad (5)$$

For building labeling, we change the query string to be of the form “A building containing r_1, r_2, \dots and r_k is called a(n) b_j .” where $r_{1..k}$ are the most informative rooms and $b_j \in L_B$ is the building label.

D. Feed-forward Approach

For the feed-forward approach, we create a single query string of the form:

$$W = \text{“This room contains } o_1, o_2, \dots \text{ and } o_k\text{.”} \quad (6)$$

This string is then fed into a language model to produce a summary embedding vector. Finally, the embedding is fed into a fine-tuned neural network head, which produces a $|L_R|$ -dimensional vector of prediction logits corresponding to the room labels, with the inferred room label being the one corresponding to the maximum value of the output:

$$\hat{r} = \arg \max_{r_j} [f_{\theta}(\Lambda(W))]_{r_j} \quad (7)$$

where $f_{\theta} : \Lambda(W) \rightarrow \mathbb{R}^{|L_R|}$ is a neural network that takes in query embeddings and outputs prediction logits and θ is its parameters and $[\cdot]_{r_j}$ indexes the element in the output vector corresponding to r_j . We choose this network to be a shallow multi-layer perceptron.

For building labeling, the queries become “This building contains r_1, r_2, \dots and r_k .” and the output space is $\mathbb{R}^{|L_B|}$.

E. Contrastive Approach

For the contrastive approach, we create and embed the same query as in the feed-forward approach in Sec. III-D. We also create and embed strings for each room label:

$$W_{r_j}^R = \text{“This room is a(n) } r_j\text{.”}, \forall r_j \in L_R \quad (8)$$

Both the language model embeddings for the query description string W and the room label strings $W_{r_j}^R$ are fed into two different fine-tuned neural networks mapping them into the same N -dimensional embedding space. Finally, the inferred room label is the one whose embedding has the highest cosine similarity with that of the query:

$$\hat{r} = \arg \max_{r_j} g_{\theta_1}(\Lambda(W)) \cdot h_{\theta_2}(\Lambda(W_{r_j}^R)) \quad (9)$$

where $g_{\theta_1}, h_{\theta_2} : \Lambda(W) \rightarrow \{\hat{v} \mid \hat{v} \in \mathbb{R}^N, \|\hat{v}\|_2 = 1\}$ are two neural networks that map language embeddings into the same space and $\theta_{1,2}$ are their respective parameters. We choose these networks to also be shallow multi-layer perceptrons.

Although this approach is fairly general, we do *not* use it for building labeling, as L_B is much sparser than L_R , meaning the label embedder would not be able to learn a general mapping that could be leveraged for novel labels.

IV. EXPERIMENTAL SETUP

A. Datasets

We evaluate the proposed algorithms on scene graphs produced from the Matterport3D dataset [40], which is commonly used in robot semantic navigation tasks [41], [42], [43]. This dataset contains regions (rooms) and contained objects, each with semantic labels and bounding boxes that we use to create scene graphs. We only look at rooms with at least one object. Objects are assigned labels from several label spaces. We consider two: mpcat40 (35 labels) and nyuClass (201 labels) [44]. In total, there are 81 buildings

with 1878 and 1866 rooms (for mpcat40 and nyuClass respectively), each with one of 23 room labels.

We divide the buildings into a 40/20/40 train/validation/test split for each label space. To produce training/validation data from rooms in those splits for our fine-tuning approaches (Sections III-D, III-E), we take the n most informative objects in each room and find all k -object permutations, producing P_k^n query datapoints per room of the form in Eq. 6, all of which correspond to the room’s label. We do this for $(k, n) \in \{(1, 2), (2, 3), (3, 4)\}$. Models trained on this data will thus be *invariant to object order and number* in the query, and can also handle less informative object labels. We generate eight such datasets by varying:

- Query embedder (RoBERTa-/BERT-large [34], [33])
- Object label space (nyuClass/mpcat40)
- Co-occurencies used for object selection (ground truth/proxy, see Sec. III-B)

Each dataset for a certain label space is produced from the same splits. All approaches and baselines are tested on the same test split. For completeness, approaches that do not require training (zero-shot and statistical baseline) are also evaluated on the entire dataset.

B. Baselines

We consider two baselines. First, we use ground-truth co-occurrence data in order to provide a *statistical baseline*. We approximate the probability of each room label as the product of the conditional probabilities of the room given each object individually (equivalent to assuming independence):

$$p(r_j | O) \approx \prod_{o_i \in O} p(r_j | o_i) \quad (10)$$

where the conditionals $p(r_j | o_i)$ are extracted from the dataset. The inferred label is thus $\arg \max_{r_j} p(r_j | O)$.

Second, we train a *GraphSage graph neural network baseline* [45] on the dataset from Sec. IV-A to predict rooms given ground truth objects. We use the 40/20/40 train/validation/test split of the dataset in Sec. IV-A.

C. Zero-shot Approach Trial Specifications

For the zero-shot approach, we vary both the ground truth/proxy object-room co-occurencies and the object label spaces for a total of four trial conditions. We test on all rooms in our datasets, choosing $k = 3$ objects per room to create the corresponding queries. For rooms containing fewer than three objects, we include as many as possible.

For all zero-shot trials, we use the GPT-J language model [35] for both evaluating query strings and generating proxy co-occurencies. Due to hardware limitations, we use the half-precision PyTorch 1.8.0 GPU release of the model [46].

D. Feed-forward Approach Trial Specifications

We train head networks on each of the eight embedding datasets. We also run two generalization experiments. First, we train the network while holding out all nyuClass datapoints whose query strings contain chairs, sinks, toilets, beds, and washing machines, then we test the trained model on these held out datapoints. This is done with ground-truth co-occurencies and RoBERTa-large as our sentence embedder.

Second, we train models with RoBERTa embeddings on mpcat40 data while *testing* on nyuClass data in order to see if they can accommodate and generalize to a different, larger input label space. In this case, we divide the mpcat40 dataset using a 80/20 training/validation split and use the entire nyuClass dataset for testing. We vary the co-occurrence generation method (ground truth and proxy).

E. Contrastive Approach Trial Specifications

We train separate head networks for embedding queries and room label strings on each of the eight embedding datasets. We use the cross entropy loss on the cosine similarity of each transformed query embedding with all transformed room label embeddings. This departs from the symmetric cross entropy loss used in [47], which assumes a one-to-one correspondence of embeddings for each batch (i.e., no two queries correspond to the same room).

We also run the two generalization experiments outlined in Sec. IV-D. Additionally, we run a third experiment wherein certain *room* labels are held out at train time, as this approach theoretically allows novel object *and* room inputs.

F. Building Trial Specifications

We extend the above formulations to also perform inference of a building’s label $\in L_B = \{\text{house, office complex, spa resort}\}$ based on the rooms within. We consider three approaches: (i) the GraphSage baseline (Sec. IV-B), but trained to predict buildings based on known objects and rooms; (ii) the zero-shot approach (Sec. III-C) with $k = 4$ and using ground-truth co-occurencies; and (iii) the feed-forward approach (Sec. III-D) with output size $|L_B| = 3$ and stochastically bootstrapped training data. We present (ii) and (iii)’s accuracies on the same test split our GNN is tested on for comparison. For completeness, we also present (ii)’s accuracy on the entire Matterport3D dataset. We do not present the contrastive approach due to building label sparseness (Sec. III-E).

G. Real Scene Graph Trial Specifications

We run the zero-shot approach to label rooms on dynamic scene graphs generated using the Hydra spatial perception system [3]. We consider three environments: a dormitory, an apartment, and an office. The object labels are noisily inferred using a fine-tuned HRNet [48] that classifies household objects into 23 labels. We consider six room labels (kitchen, bathroom, hallway, lounge, stairwell, and bedroom) while using proxy co-occurencies to pick query objects. All rooms with at least one object are evaluated.

V. RESULTS

A. Zero-shot Approach Results

The zero-shot trials yield inference accuracies of 27.26 – 52.57% when run on the entire dataset (see parenthesized values in Table I). The ground-truth co-occurrence trials perform better than the statistical baseline evaluated on the whole dataset, which also uses ground truth frequencies. No trial outperforms the GraphSage baseline, but the latter requires training and cannot be easily extended to additional labels, unlike our approach (by virtue of being zero-shot).

TABLE I
TEST SPLIT ACCURACIES FOR ALL APPROACHES (FULL DATASET ACCURACIES IN PARENTHESES)

	Baseline		Zero-shot		Feed-forward				Contrastive				
	Statistical		GraphSage	GT	Proxy	RoBERTa		BERT		RoBERTa		BERT	
	GT	Proxy	GT	Proxy	GT	Proxy	GT	Proxy	GT	Proxy	GT	Proxy	
nyuClass	52.74% (50.64%)	64.15%	52.20% (52.57%)	27.24% (28.24%)	65.42%	56.21%	64.62%	55.41%	65.69%	57.14%	63.95%	53.27%	
mpcat40	44.71% (46.86%)	59.13%	48.86% (50.05%)	27.45% (27.26%)	59.57%	54.16%	59.19%	56.68%	60.20%	57.18%	59.70%	54.79%	

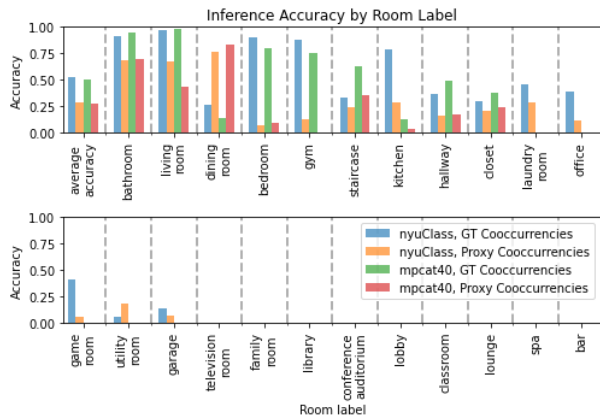


Fig. 4. Zero-shot accuracies on all data for all conditions, by room label.

Our algorithm achieves high accuracies for several common household rooms (bathroom, bedroom, kitchen, and living room). For the best performing trial, nyuClass with ground-truth co-occurrences, accuracies for these key rooms range from 79.22 – 97.14% (see Fig. 4). There also are two trends for when a room will *not* be classified correctly:

- **Room lacks disambiguating objects:** Bathrooms and bedrooms have objects almost exclusive to them (e.g., toilets and beds), but rooms like lobbies and family rooms only contain more ubiquitous ones (tables, chairs, etc), and so are harder to identify.
- **Room is not “standard”:** Bars, libraries, and spas all more commonly refer to *buildings*, not rooms. Thus, queries for those rooms are scored worse than ones that are unambiguously rooms. Gyms could also count, but they have disambiguating objects (gym equipment).

For the other rooms, the language model shows the desired common sense when classifying them. Our approach also demonstrates zero-shot generalization, handling the smaller, 35-object label space (mpcat40) *and* the much larger, 201-object label space (nyuClass). In fact, the nyuClass trials result in higher accuracies than their mpcat40 counterparts when evaluated on the whole dataset (see Table I), as nyuClass’s labels are more specific and informative. This benefit is best shown in the following cases:

- **Kitchens and laundry rooms:** Both rooms are characterized by appliances. While nyuClass provides fine-grained labels (e.g., washing machine vs. stoves), mpcat40 groups all those objects under the broad and ambiguous category of “appliances,” making differentiation of the two room labels difficult.
- **Game rooms and garages:** Game rooms are characterized by recreational objects, like ping-pong/foosball tables. Both appear in nyuClass, but are just labeled

as “tables” by mpcat40, making these rooms easier to identify when using nyuClass. Likewise, garage doors (nyuClass) are classified as just “doors” in mpcat40.

Finally, all trials take ~ 1.18 seconds to infer a room’s label, with most of the overhead being language model evaluations.

B. Feed-forward and Contrastive Approaches Results

The feed-forward approach achieves 54.16 – 65.42% test accuracy, beating the statistical baseline (46.86 – 52.74%) and the zero-shot approach (27.24 – 52.20%) in all conditions (Table I). Notably, unlike for the zero-shot case, this is even true for the conditions when using proxy co-occurrences, so the model does not explicitly need ground-truth co-occurrences for picking out objects to achieve high performance (though some is still required for training). The contrastive approach yields similar results, still outperforming the zero-shot case and statistical baseline in all conditions. All fine-tuning trials that use ground-truth co-occurrences yield similar/slightly higher results than the corresponding GraphSage baseline, while the proxy trials are still competitive. Lastly, both approaches use one language model evaluation per inference, compared to $|L_R|$ for zero-shot. The head networks are also shallow, so these approaches run faster than the zero-shot approach.

C. Fine-tuned Generalization Results

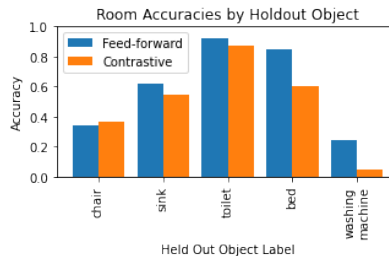


Fig. 5. Test accuracies for rooms containing each of the holdout objects.

Using language models to embed the query room descriptions enables generalization to novel object classes. Both fine-tuning approaches do well for some objects in the hold-out object trials (see Fig. 5). Even when they do not appear in training, both approaches correctly classify rooms whose queries contain sinks, toilets, and beds between 54.79 – 92.4% of the time. *This indicates zero-shot generalization abilities.* Our fine-tuned networks likely learned to extract essential information on room labels from query embeddings containing only non-held out objects that generalizes to the held out ones. For instance, while toilets are held out, other related bathroom objects, like bathtubs, are not. Due to their

REFERENCES

- [1] S. Bowman, N. Atanasov, K. Daniilidis, and G. Pappas, "Probabilistic data association for semantic SLAM," in *IEEE Intl. Conf. on Robotics and Automation (ICRA)*, 2017, pp. 1722–1729.
- [2] A. Rosinol, A. Violette, M. Abate, N. Hughes, Y. Chang, J. Shi, A. Gupta, and L. Carlone, "Kamera: From SLAM to spatial perception with 3D dynamic scene graphs," *Intl. J. of Robotics Research*, vol. 40, no. 12–14, pp. 1510–1546, 2021, arXiv preprint arXiv: 2101.06894, (pdf).
- [3] N. Hughes, Y. Chang, and L. Carlone, "Hydra: a real-time spatial perception engine for 3D scene graph construction and optimization," in *Robotics: Science and Systems (RSS)*, 2022, (pdf).
- [4] W. von Humboldt, P. Heath, and H. Aarsleff, *On Language: The Diversity of Human Language-Structure and its Influence on the Mental Development of Mankind*, ser. Texts in German Philosophy. Cambridge University Press, 1988. [Online]. Available: <https://books.google.com/books?id=0CXEQwAACAAJ>
- [5] N. Chomsky, *Aspects of the Theory of Syntax*. Cambridge: The MIT Press, 1965. [Online]. Available: <http://www.amazon.com/Aspects-Theory-Syntax-Noam-Chomsky/dp/0262530074>
- [6] J. Dong, X. Fei, and S. Soatto, "Visual-Inertial-Semantic scene representation for 3D object detection," in *IEEE Conf. on Computer Vision and Pattern Recognition (CVPR)*, 2017.
- [7] L. Nicholson, M. Milford, and N. Sünderhauf, "QuadricSLAM: Dual quadrics from object detections as landmarks in object-oriented SLAM," *IEEE Robotics and Automation Letters*, vol. 4, pp. 1–8, 2018.
- [8] K. Ok, K. Liu, and N. Roy, "Hierarchical object map estimation for efficient and robust navigation," in *2021 IEEE International Conference on Robotics and Automation (ICRA)*, 2021, pp. 1132–1139.
- [9] J. Behley, M. Garbade, A. Milioto, J. Quenzel, S. Behnke, C. Stachniss, and J. Gall, "SemanticKITTI: A Dataset for Semantic Scene Understanding of LiDAR Sequences," in *Intl. Conf. on Computer Vision (ICCV)*, 2019.
- [10] M. Grinvald, F. Furrer, T. Novkovic, J. J. Chung, C. Cadena, R. Siegwart, and J. Nieto, "Volumetric Instance-Aware Semantic Mapping and 3D Object Discovery," *IEEE Robotics and Automation Letters*, vol. 4, no. 3, pp. 3037–3044, 2019.
- [11] R. Rosu, J. Quenzel, and S. Behnke, "Semi-supervised semantic mapping through label propagation with semantic texture meshes," *Intl. J. of Computer Vision*, 06 2019.
- [12] C. Li, H. Xiao, K. Tateno, F. Tombari, N. Navab, and G. D. Hager, "Incremental scene understanding on dense SLAM," in *IEEE/RSJ Intl. Conf. on Intelligent Robots and Systems (IROS)*, 2016, pp. 574–581.
- [13] J. McCormac, R. Clark, M. Bloesch, A. Davison, and S. Leutenegger, "Fusion++: Volumetric object-level SLAM," in *Intl. Conf. on 3D Vision (3DV)*, 2018, pp. 32–41.
- [14] J.-R. Ruiz-Sarmiento, C. Galindo, and J. Gonzalez-Jimenez, "Building multiversal semantic maps for mobile robot operation," *Knowledge-Based Systems*, vol. 119, pp. 257–272, 2017.
- [15] C. Galindo, A. Saffiotti, S. Coradeschi, P. Buschka, J. Fernández-Madrigal, and J. González, "Multi-hierarchical semantic maps for mobile robotics," in *IEEE/RSJ Intl. Conf. on Intelligent Robots and Systems (IROS)*, 2005, pp. 3492–3497.
- [16] C. Lu, R. Krishna, M. Bernstein, and F.-F. Li, "Visual relationship detection with language priors," in *European Conference on Computer Vision*, 2016, pp. 852–869.
- [17] J. Johnson, A. Gupta, and L. Fei-Fei, "Image generation from scene graphs," in *IEEE Conf. on Computer Vision and Pattern Recognition (CVPR)*, 2018.
- [18] I. Armeni, Z. He, J. Gwak, A. Zamir, M. Fischer, J. Malik, and S. Savarese, "3D scene graph: A structure for unified semantics, 3D space, and camera," in *Intl. Conf. on Computer Vision (ICCV)*, 2019, pp. 5664–5673.
- [19] A. Rosinol, A. Gupta, M. Abate, J. Shi, and L. Carlone, "3D dynamic scene graphs: Actionable spatial perception with places, objects, and humans," in *Robotics: Science and Systems (RSS)*, 2020, (pdf), (media), (video). [Online]. Available: <http://news.mit.edu/2020/robots-spatial-perception-0715>
- [20] M. Yasunaga, H. Ren, A. Bosselut, P. Liang, and J. Leskovec, "Qa-gnn: Reasoning with language models and knowledge graphs for question answering," 2021. [Online]. Available: <https://arxiv.org/abs/2104.06378>
- [21] F. Petroni, T. Rocktäschel, P. Lewis, A. Bakhtin, Y. Wu, A. H. Miller, and S. Riedel, "Language models as knowledge bases?" 2019.
- [22] F. Petroni, P. Lewis, A. Piktus, T. Rocktäschel, Y. Wu, A. H. Miller, and S. Riedel, "How context affects language models' factual predictions," in *Automated Knowledge Base Construction*, 2020. [Online]. Available: <https://openreview.net/forum?id=025X0zPfn>
- [23] A. Creswell, M. Shanahan, and I. Higgins, "Selection-inference: Exploiting large language models for interpretable logical reasoning," 2022. [Online]. Available: <https://arxiv.org/abs/2205.09712>
- [24] S. Tellex, T. Kollar, S. Dickerson, M. R. Walter, A. G. Banerjee, S. J. Teller, and N. Roy, "Understanding natural language commands for robotic navigation and mobile manipulation," in *AAAI*, 2011. [Online]. Available: <http://www.aaai.org/ocs/index.php/AAAI/AAAI11/paper/view/3623>
- [25] P. Sharma, B. Sundaralingam, V. Blukis, C. Paxton, T. Hermans, A. Torralba, J. Andreas, and D. Fox, "Correcting robot plans with natural language feedback," 2022. [Online]. Available: <https://arxiv.org/abs/2204.05186>
- [26] C. Lynch and P. Sermanet, "Language conditioned imitation learning over unstructured data," 2020. [Online]. Available: <https://arxiv.org/abs/2005.07648>
- [27] M. Shridhar, L. Manuelli, and D. Fox, "Cliport: What and where pathways for robotic manipulation," 2021. [Online]. Available: <https://arxiv.org/abs/2109.12098>
- [28] T. Kollar, S. Tellex, D. K. Roy, and N. Roy, "Toward understanding natural language directions," in *HRI 2010*, 2010.
- [29] T. M. Howard, S. Tellex, and N. Roy, "A natural language planner interface for mobile manipulators," in *2014 IEEE International Conference on Robotics and Automation (ICRA)*, 2014, pp. 6652–6659.
- [30] C. Matuszek, E. Herbst, L. Zettlemoyer, and D. Fox, *Learning to Parse Natural Language Commands to a Robot Control System*. Heidelberg: Springer International Publishing, 2013, pp. 403–415. [Online]. Available: https://doi.org/10.1007/978-3-319-00065-7_28
- [31] M. Ahn, A. Brohan, N. Brown, Y. Chebotar, O. Cortes, B. David, C. Finn, K. Gopalakrishnan, K. Hausman, A. Herzog, D. Ho, J. Hsu, J. Ibarz, B. Ichter, A. Irpan, E. Jang, R. J. Ruano, K. Jeffrey, S. Jesmonth, N. J. Joshi, R. Julian, D. Kalashnikov, Y. Kuang, K.-H. Lee, S. Levine, Y. Lu, L. Luu, C. Parada, P. Pastor, J. Quiambao, K. Rao, J. Rettinghouse, D. Reyes, P. Sermanet, N. Sievers, C. Tan, A. Toshev, V. Vanhoucke, F. Xia, T. Xiao, P. Xu, S. Xu, and M. Yan, "Do as i can, not as i say: Grounding language in robotic affordances," 2022. [Online]. Available: <https://arxiv.org/abs/2204.01691>
- [32] D. Chaves, J. Ruiz-Sarmiento, N. Petkov, and J. González-Jiménez, "From object detection to room categorization in robotics," 01 2020, pp. 1–6.
- [33] J. Devlin, M.-W. Chang, K. Lee, and K. Toutanova, "Bert: Pre-training of deep bidirectional transformers for language understanding," 2019.
- [34] Y. Liu, M. Ott, N. Goyal, J. Du, M. Joshi, D. Chen, O. Levy, M. Lewis, L. Zettlemoyer, and V. Stoyanov, "RoBERTa: A robustly optimized BERT pretraining approach," 2019. [Online]. Available: <https://arxiv.org/abs/1907.11692>
- [35] B. Wang and A. Komatsuzaki, "GPT-J-6B: A 6 Billion Parameter Autoregressive Language Model," <https://github.com/kingoflolz/mesh-transformer-jax>, May 2021.
- [36] S. Black, L. Gao, P. Wang, C. Leahy, and S. Biderman, "GPT-Neo: Large Scale Autoregressive Language Modeling with Mesh-Tensorflow," Mar. 2021, If you use this software, please cite it using these metadata. [Online]. Available: <https://doi.org/10.5281/zenodo.5297715>
- [37] A. Radford, J. Wu, R. Child, D. Luan, D. Amodei, and I. Sutskever, "Language models are unsupervised multitask learners," 2019.
- [38] J. Salazar, D. Liang, T. Q. Nguyen, and K. Kirchhoff, "Masked language model scoring," in *Proceedings of the 58th Annual Meeting of the Association for Computational Linguistics*, 2020. [Online]. Available: <https://doi.org/10.18653/v1/2020.acl-main.240>
- [39] F. Barbieri, L. E. Anke, and J. Camacho-Collados, "Xlm-t: Multilingual language models in twitter for sentiment analysis and beyond," 2021. [Online]. Available: <https://arxiv.org/abs/2104.12250>
- [40] A. Chang, A. Dai, T. Funkhouser, M. Halber, M. Niessner, M. Savva, S. Song, A. Zeng, and Y. Zhang, "Matterport3d: Learning from rgb-d data in indoor environments," *International Conference on 3D Vision (3DV)*, 2017.
- [41] Manolis Savva*, Abhishek Kadian*, Oleksandr Maksymets*, Y. Zhao, E. Wijmans, B. Jain, J. Straub, J. Liu, V. Koltun, J. Malik, D. Parikh, and D. Batra, "Habitat: A Platform for Embodied AI Research," in *Proceedings of the IEEE/CVF International Conference on Computer Vision (ICCV)*, 2019.

- [42] K. Yadav, S. K. Ramakrishnan, J. Turner, A. Gokaslan, O. Maksymets, R. Jain, R. Ramrakhya, A. X. Chang, A. Clegg, M. Savva, E. Undersander, D. S. Chaplot, and D. Batra, “Habitat challenge 2022,” <https://aihabitat.org/challenge/2022/>, 2022.
- [43] A. Szot, A. Clegg, E. Undersander, E. Wijmans, Y. Zhao, J. Turner, N. Maestre, M. Mukadam, D. Chaplot, O. Maksymets, A. Gokaslan, V. Vondrus, S. Dharur, F. Meier, W. Galuba, A. Chang, Z. Kira, V. Koltun, J. Malik, M. Savva, and D. Batra, “Habitat 2.0: Training home assistants to rearrange their habitat,” in *Advances in Neural Information Processing Systems (NeurIPS)*, 2021.
- [44] P. K. Nathan Silberman, Derek Hoiem and R. Fergus, “Indoor segmentation and support inference from rgbd images,” in *ECCV*, 2012.
- [45] W. L. Hamilton., R. Ying, and J. Leskovec, “Inductive representation learning on large graphs,” in *Advances in Neural Information Processing Systems (NIPS)*, Dec. 2017, p. 1025–1035.
- [46] A. Paszke, S. Gross, F. Massa, A. Lerer, J. Bradbury, G. Chanan, T. Killeen, Z. Lin, N. Gimelshein, L. Antiga, A. Desmaison, A. Kopf, E. Yang, Z. DeVito, M. Raison, A. Tejani, S. Chilamkurthy, B. Steiner, L. Fang, J. Bai, and S. Chintala, “Pytorch: An imperative style, high-performance deep learning library,” in *Advances in Neural Information Processing Systems 32*. Curran Associates, Inc., 2019, pp. 8024–8035. [Online]. Available: <http://papers.neurips.cc/paper/9015-pytorch-an-imperative-style-high-performance-deep-learning-library.pdf>
- [47] A. Radford, J. W. Kim, C. Hallacy, A. Ramesh, G. Goh, S. Agarwal, G. Sastry, A. Askell, P. Mishkin, J. Clark, G. Krueger, and I. Sutskever, “Learning transferable visual models from natural language supervision,” 2021. [Online]. Available: <https://arxiv.org/abs/2103.00020>
- [48] J. Wang, K. Sun, T. Cheng, B. Jiang, C. Deng, Y. Zhao, D. Liu, Y. Mu, M. Tan, X. Wang, W. Liu, and B. Xiao, “Deep high-resolution representation learning for visual recognition,” *IEEE Transactions on Pattern Analysis and Machine Intelligence*, vol. 43, no. 10, pp. 3349–3364, 2021.
- [49] D. P. Kingma and J. Ba, “Adam: A method for stochastic optimization,” 2017.

APPENDIX

A. Converting Matterport3D to Scene Graphs

To convert semantic meshes from Matterport3D into scene graphs, we create a node for each region and object [40]. Then, we connect all object nodes assigned to a region to that region’s room node. We also filter out some regions. While Matterport3D contains outdoor regions as well (“yard,” “balcony,” and “porch”), we do not perform inference over them, since they are not true rooms and thus would require an alternate query string structure. In addition to outdoor regions, we also remove all rooms with no objects within or with the label “none.”

Each object is assigned labels from several label spaces. We consider the original labels used by Matterport3D (mpcat40) and the labels used by NYU (nyuClass) [44]. For both, we filter out nodes belonging to the mpcat40 categories “ceiling,” “wall,” “floor,” “miscellaneous,” “object,” and any other unlabeled nodes. We remove these categories because they are either not objects within the room or they are ambiguous to the point of being semantically uninformative. However, for nyuClass, we do *not* reject objects classified by mpcat40 as “object,” since nyuClass has many more fine-grained and semantically-rich categories which all are mapped to this category. After pre-processing the label spaces in this way, mpcat40 has 35 object labels and nyuClass has 201. Both datasets share a room label space with 23 labels. See Table IV for a breakdown of room label frequencies.

We perform a few additional dataset pre-processing steps to produce the final scene graph dataset with 1878 rooms. First, since some objects are assigned an incorrect region

TABLE IV
ROOM LABEL FREQUENCIES IN PRE-PROCESSED DATASET

Room Label	Bar	Bathroom	Bedroom	Classroom	Closet	Conference Auditorium
Occurrences	3	365	251	2	99	16
Percentage	0.16%	19.43%	13.37%	0.11%	5.27%	0.85%
Room Label	Dining Room	Family Room	Game Room	Garage	Gym	Hallway
Occurrences	74	61	17	14	16	326
Percentage	3.94%	3.25%	0.91%	0.75%	0.85%	17.36%
Room Label	Kitchen	Laundry Room	Library	Living Room	Lobby	Lounge
Occurrences	78	35	1	71	62	64
Percentage	4.15%	1.86%	0.05%	3.78%	3.30%	3.41%
Room Label	Office	Spa	Staircase	Television Room	Utility Room	Total
Occurrences	98	44	152	13	16	1878
Percentage	5.22%	2.34%	8.09%	0.69%	0.85%	100%

(e.g., toilets are assigned to living rooms, despite (i) that being non-sensible and (ii) the toilet not being within the bounding box of the living room), we check to see if each object is within the bounding box of its assigned region. If not, then it is re-assigned to whichever region’s bounding box contains it, and the corresponding scene-graph connection is also made. Second, nyuClass has some misspelled labels (e.g., “refridgerator” instead of “refrigerator”), so we correct all of those too. Lastly, sometimes, a single nyuClass label may be erroneously assigned to multiple mpcat40 labels. This is most problematic when one of the mpcat40 labels is rejected and the other is not. To address this, we use the first mpcat40 label for each nyuClass label that is *not* rejected (e.g., nyuClass label “stairs” is mapped to mpcat40 “miscellaneous,” which is rejected, and “stairs,” which is not, so we keep the latter). However, this means some labels which *should* be rejected are not rejected, so we also manually filter out all nyuClass object labels that are the *same* as those of rejected mpcat40 labels: “ceiling,” “floor,” and “wall”.

B. Building Feed-forward Data Generation Details

To generate data for inferring building labels via the feed-forward approach, for each building in the train set, we sample (without replacement) and shuffle $k = 4$ rooms out of the present ones, subsequently putting them into query strings, which we then embed via language model. The probability of choosing each room is proportional to the number of times that room appears in the building. We do this 1000 times total for each room, meaning the training dataset label distribution has the same ratios as the training dataset used by GraphSage.

C. Training Hyperparameters

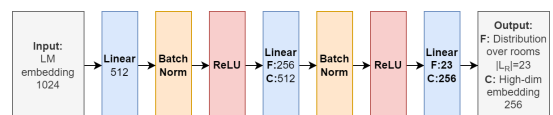


Fig. 7. The fine-tuned feed-forward and contrastive heads use the same architecture, but with different number of neurons for certain layers (reported under **F**: and **C**: respectively).

For the *GraphSage baseline*, we train for 500 epochs with a learning rate of $5e-3$, weight decay of $1e-4$, hidden state dimension of 16, dropout of 0.2, and 2 iterations of message-passing. For the *feed-forward approach*, we train each network for 200 epochs with a batch size of 512 using cross entropy loss via the Adam optimizer with a learning rate of $1e-4$, $\beta_1, \beta_2 = 0.9, 0.999$, weight decay of $1e-3$, and a StepLR scheduler with step size of 10 and $\gamma=0.5$ [49]. For the *contrastive approach*, we train each network for 200 epochs with a batch size of 512 using the Adam optimizer with a learning rate of $1e-5$, $\beta_1, \beta_2 = 0.9, 0.999$, weight decay factor of $1e-3$, and a StepLR scheduler with step size of 20 and $\gamma=0.9$. The fine-tuned networks' architectures are shown in Fig. 7.